

Synthetic Zooming of Tomographic Images by Combination of Lattices

Neha Dixit, N.V.Kartheek M and Jayanthi Sivaswamy

Abstract—We propose a method for synthetic zooming of tomographic images by applying super resolution technique on reconstructed data via a union of rotated lattices (URL). The proposed method consists of two steps: (i) sinogram data is filtered and backprojected on to two lattices, which are rotated versions of each other and (ii) the samples from the two lattices are interpolated to generate the upsampled image. Square and hexagonal lattices have been investigated for URL. Results of subjective and objective evaluations of the proposed method on analytic phantoms are presented and compared with direct upsampling of data reconstructed on a single square lattice and upsampled image generated by union of low resolution shifted images (USL). The proposed method shows qualitative and quantitative improvement over direct upsampling but when compared with USL, generated upsampled images are of comparable quality.

Index Terms—Super-resolution, Tomographic images, Combination of rotated lattices.

I. INTRODUCTION

IMPROVING the resolution of tomographic images has been an active area of research in the past few years. One can obtain high resolution images by increasing the number of detectors and views which will result in increased X-ray dosage (for CT) and scan time (for PET/SPECT). Reconstruction based on a union of shifted lattice [1] is an alternative method which increases the resolution of tomographic images without altering the number of detectors.

Super resolution (SR) techniques based on a combination of a set of low resolution images with spatial shifts have been examined for CT [2] and PET [3] [4] [5] images. Ideally, k times upsampled image is generated by combining, k^2 subpixel shifted images. This idea was implemented in [3] to generate PET images by acquiring multiple low resolution images sequentially, after translating or rotating the same object (or detector array) by a subpixel distance with respect to the previous acquisition. Though this demonstrated the SR concept clearly, it was by directly applying the shifts and rotations to a phantom. In the case of a real patient, this is practically not attractive as it will increase the scan duration and it can also potentially increase the probability of patient motion during scan. Hence, an alternative was proposed in [4] that tried to achieve the sub-pixel shifts in the reconstruction space. Specifically, it was shown that it is possible to generate the desired low resolution images by introducing shifts in the reconstruction grids using the same sinogram data. An improvement on this by way of a reduction in the required



Fig. 1: Processing stages in filtered back projection

number of low resolution images, with no degradation in the quality of the final image, was investigated in [5]. Two new algorithms, namely ISR-1 (incomplete super resolution) and ISR-2, were presented which require only $2k - 1$ and k low resolution images respectively instead of the standard k^2 images.

In general, the concept of super resolution relies on using a combination of low resolution images which provide a *different view* of an object/scene. Translation and rotation are the possible ways in which these *different views* can be obtained. Though both were demonstrated by [3] by directly manipulating a phantom, the methods in [4] and [5] have only focused on translation by sub-pixel shifts. We examine the rotation alternative in this paper and propose a solution for synthetically zooming tomographic images by combining samples from *two* low resolution images which are rotated versions of each other. These low resolution images, as in [4], can be derived from the same sinogram data. We investigate if this alternative has any implications on SR image reconstruction in terms of the number of images required for a given upsampling factor and the final image quality. For simplicity, the remaining part of this paper will assume parallel beam tomography and reconstruction by filtered back projection (FBP) [9] and ordered subset expectation maximization (OSEM) [12].

II. METHOD

Let $I(x, y)$ be the imaged object and $P(r, \theta)$ be the corresponding sinogram data where (r, θ) are both discrete. The process of reconstruction as described in [4] consists of two main steps: back-projection of $P(r, \theta)$ into a continuous image $I_{R_c}(x, y)$ and sampling it to generate a digital image $I_R[n1, n2]$ where $[n1, n2]$ are discrete. Algorithm used for implementing FBP is given in Fig.1.

Assuming the image $I_R[n1, n2]$ is of size $M \times M$, in order to up-sample this image by a factor of k , the traditional approach is to introduce $(k - 1)$ zeros row- and column-wise and interpolate between the non-zero valued samples. The limitation with this approach is that the result entirely depends on the choice of the interpolation kernel as no new data has actually been used to derive the required new samples. In SR

techniques, non-overlapping sets of samples from $I_{R_c}(x, y)$ are derived and then interpolated such as in union of shifted lattices [1]. We generate these desired sets by sampling

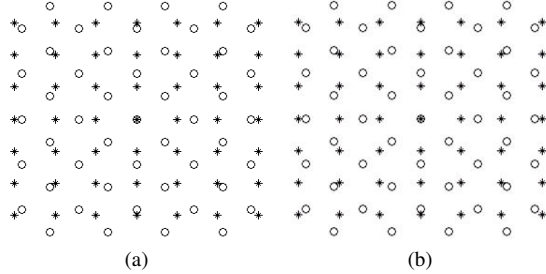


Fig. 2: Sample points drawn from a union of rotated lattices: (a) S (indicated by $*$) and S_{45} (indicated by o) and (b) H (indicated by $*$) and H_{30} (indicated by o).

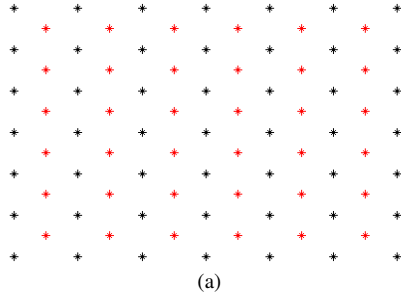


Fig. 3: Sample points drawn from a union of shifted lattices centered at $(0, 0)$ and $(1/2, 1/2)$

$I_{R_c}(x, y)$ with two lattices which are rotated versions of each other. Consider 2×2 sampling matrices V and $V_\phi = A_\phi V$, where A_ϕ is a rotation matrix. The desired sets of samples I_R and I_{R_ϕ} are then given as

$$I_R[n] = I_{R_c}(Vn) \quad (1)$$

$$I_{R_\phi}[n] = I_{R_c}(V_\phi n) \quad (2)$$

where $n = [n_1, n_2]^T$. The samples obtained by combining the samples from I_R and I_{R_ϕ} are shown in Fig.2(a) for $\phi = 45^\circ$. In the preceding formulation, the sampling matrix V will vary with the choice of the underlying lattice, namely square or hexagonal. Hexagonal lattices offer superior packing efficiency with non-orthogonal bases [6], [7] and hence have been considered in our work. The sample points derived from a combination of hexagonal lattices are shown in Fig.2(b) for $\phi = 30^\circ$. From these figures, an interesting point can be observed. The union operation on the two rotated lattices breaks up the periodicity and hence the result is in a non-uniformly sampled space. However, there is some quasi-periodicity in this space. This is in contrast to the samples in union of shifted lattices, where they always lie in a periodic lattice. For example, Fig.3 shows samples obtained from a union of a square lattice and another shifted diagonally by half a pixel. The periodicity present here can be contrasted

with the union of rotated (by 45°) square lattices in Fig.2(a) where it is absent.

Given a sinogram data $P(r, \theta)$, we first reconstruct two images, namely I_R and I_{R_ϕ} using FBP and Equations 1 and 2. Next, we derive an upsampled (by k) image denoted as URL^k by interpolating between the samples as follows:

$$URL^k = (I_R + I_{R_\phi}) * h \quad (3)$$

where $*$ denotes convolution and h is an interpolating function. Since two different lattices were considered in our work, the results obtained with the square and hexagonal lattices are denoted as URL_{sq}^k and URL_{hex}^k respectively.

For validation, the results of the proposed method are compared with two types of images :

- a) Direct upsampled images S^k : Obtained by upsampling I_R via bicubic interpolation kernel.
- b) Union of shifted lattices USL^k : The upsampled (by k) result obtained by combining low resolution shifted images.

III. IMPLEMENTATION

1) *Generating URL images*: Since, combination of rotated lattices generates quasi-periodic samples, thin plate splines were chosen to interpolate between them and generate the desired samples on upsampled lattice. The computed samples were always defined to be on a square lattice regardless of the original (low resolution) lattices. The angle of rotation ϕ was taken to be 45° and 30° for square and hexagonal lattices, respectively, to minimize overlap between I_R and I_{R_ϕ} sample points. Hexagonal lattice with basis vectors $(1, 0)$, $(1/\sqrt{3}, 1)$ and $(1, 1/\sqrt{3})$, $(0, 1)$ was used to generate a good distribution of samples. Up-sampling factors of $k = 2, 4$ and 6 were considered in our experiments. In all cases, the input samples were drawn only from two rotated lattices. This was done in order to study the degradation in quality as the sampling factor was increased.

2) *Generating USL images*: Ideally for an upsampling factor of k , k^2 subpixel shifted images are needed to generate high resolution image. It has been shown in [5] that high resolution images of similar quality can be obtained by combining just k subpixel diagonal shifted images. Hence, diagonal shifted low resolution images were reconstructed with the FBP algorithm using Fessler's toolbox [12]. Samples from these images were interpolated using a bicubic kernel to generate desired samples on a high resolution grid (upsampled image) using Vanderwalle's toolbox [11].

3) *OSEM*: The quality of tomographic images are adversely affected by the introduction of noise during the acquisition process. For PET/SPECT imaging, the strength of the detected signal (projection or sinogram data) is very weak compared to CT and MR images which results in poor resolution (typically 128×128) and decrease in SNR (signal to noise ratio) of the reconstructed images. Traditional iterative methods like maximum likelihood - expectation maximization (ML-EM) or ordered subsets expectation maximization (OSEM) are used for improving the image quality. OSEM uses FBP generated image as an initial estimate, and improves the quality iteratively [12]. Some of the results in our experiment

were generated using the OSEM reconstruction algorithm (with 21 subsets and 2 iterations) implementation in the Fessler's toolbox.

In CT imaging there are two types of noise, one is electrical noise or roundoff error which can be modeled as additive noise and other is shot noise which can be modeled as Poisson distribution [10]. In the case of PET imaging, shot noise is prominent [9]. We assume sufficiently large mean for the Poisson noise and hence approximate it with a Gaussian distribution. Thus, for generating the sinogram data suitable for both the modalities, additive Gaussian noise (0 mean, standard deviation =0.001) was added to the analytical sinogram.

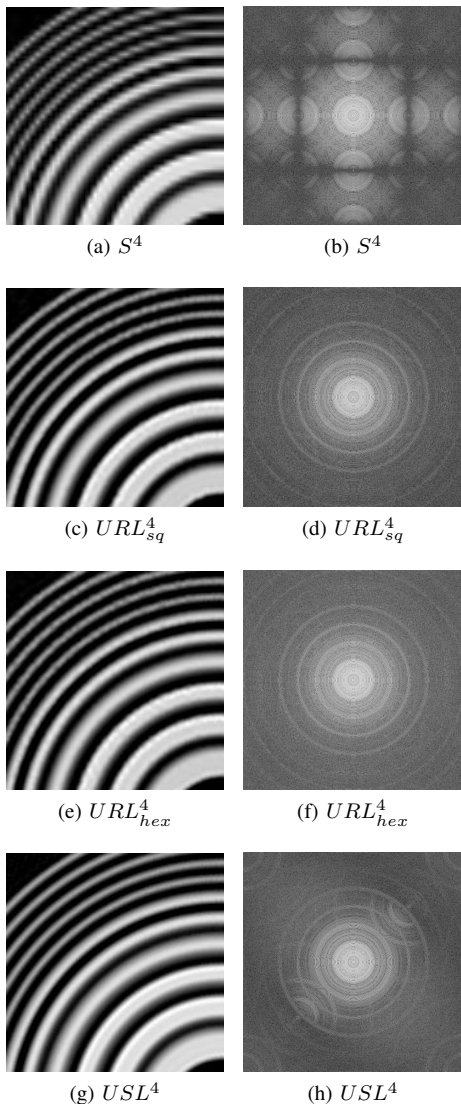
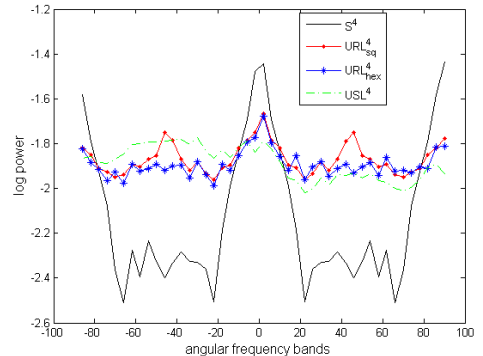


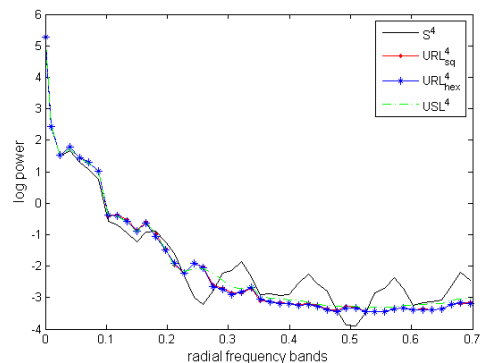
Fig. 4: Upsampled results for Concentric rings (only 1 quadrant is shown) and the corresponding full amplitude spectra.

IV. RESULTS

Three analytically generated phantoms were used to study the effects of upsampling samples from a union of rotated lattices: The concentric rings and lines phantoms were used to study preservation of curved and linear structures respectively;



(a) Angular energy plot



(b) Radial energy plot

Fig. 5: Angular and radial energy plot of concentric rings for different upsampling methods

The dots phantom was used to compare the contrast and spatial resolution of the up-sampled image. The results of the experiments were compared quantitatively using intensity (along a line) profiles, energy distribution in angular and radial directions, and noise profiles. Intensity profiles help to compare the contrast difference between the images.

A. Concentric rings

A concentric rings phantom was generated analytically and used to study the preservation of curved structure in the up-sampled image and the effectiveness of an up-sampling method in suppressing imaging. Images were reconstructed from sinogram of size 151×180 by implementing the FBP algorithm. Fig.4 (a), (c), (e) and (g) show one quadrant of the up-sampled S^4 , URL_{sq}^4 , URL_{hex}^4 and USL^4 images (up-sampling factor 4) of the concentric rings phantom while (b), (d), (f) and (h) show their corresponding full amplitude spectra. While up-sampling an image, our aim is to preserve details and definition of the image but prevent imaging. From the spectra, one can observe the prominent imaging present in the S and USL results and not in URL . It is evident however, that union of lattices (shifted or rotated) helps in preserving the definition of curves. The S image exhibits aliasing and distortion that is typical of direct upsampling. The energy distribution, computed from the normalized power spectrum of an image [8], in angular (-90° to 90° in steps of 4°) direction is shown in Fig.5(a) and radial ($\rho = 64$ bands) direction is

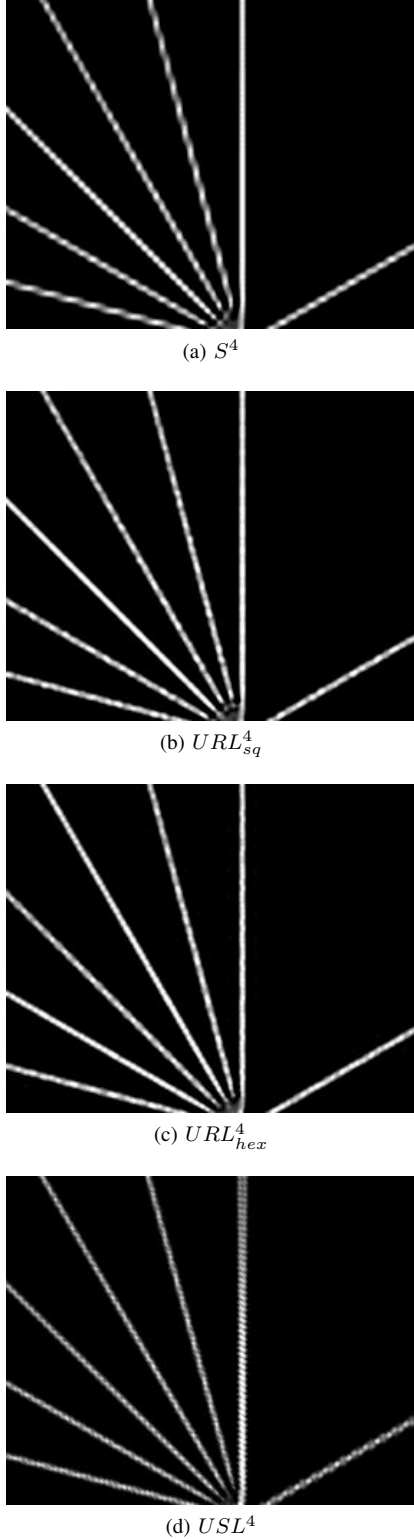


Fig. 6: Upsampled results for Lines

shown in Fig.5(b). The energy variation across ρ is seen to be much smoother for USL and URL compared to S due to reduction in imaging. On an average, there is a boost in energy for all angles over URL_{hex} with a directional bias evident at 45° for URL_{sq} . USL images shows prominent increase of energy from -90° to 0° compared to URL.

B. Lines

Lines phantom was used to study the preservation of linear structures by different methods of upsampling. Images are reconstructed from sinogram of size 121×180 using the FBP algorithm. The quality of the images was evaluated visually. Fig.6 (a), (b), (c) and (d) show the up-sampled S^4 , URL_{sq}^4 , URL_{hex}^4 and USL^4 images (up-sampling factor 4) of the lines at angles 30° 90° , 105° , 120° , 135° , 150° and 165° . All the lines are crisper and well defined in URL images compared to USL and S images. In the USL result, the vertical line exhibits blurring towards the periphery of the image even though this grid supports a good representation for a line at 90° . In the S image, distortion is present in all the lines except for vertical one Fig. 6(a).

C. Dots

The dots phantom was created to compare the contrast and spatial resolution of the up-sampled image using line profiles and contrast ratio. Images are reconstructed from a noisy sinogram of size 101×180 by implementing FBP and OSEM. Fig.7 (a), (b), (c) and (d) show the up-sampled S^4 , URL_{sq}^4 , URL_{hex}^4 and USL^4 images reconstructed using FBP. OSEM has been implemented to improve the SNR of the reconstructed image. OSEM generated upsampled images are shown in Fig.8 (a) through (c). Fig.10 (a), (b) and (c) show the ROI of up-sampled S^6 , URL_{sq}^6 and USL^6 images reconstructed using OSEM.

Visually, URL_{sq} appears noisier than URL_{hex} and USL . This is partially due to the fact that the latter are of similar quality but with higher contrast.

TABLE I: Contrast ratio across last two lines of the Dots Phantom

Images	FBP		OSEM			
	k=4		k=4		k=6	
	second last	last	second last	last	second last	last
S^4	0.5406	0.6086	0.5801	0.7036	0.5752	0.6964
USL^4	0.5645	0.6516	0.6235	0.7730	0.6153	0.7861
URL_{sq}^4	0.5717	0.6638	0.6326	0.7441	0.6273	0.7527
URL_{hex}^4	0.5581	0.6534	-	-	-	-

A quantitative evaluation of the contrast was carried out by taking the intensity profile in the last 2 lines of the image and using the contrast ratio [5] defined as follows.

$$CR = \frac{\frac{1}{m} \sum_{i=1}^m P_i - \frac{1}{n} \sum_{j=1}^n T_j}{\frac{1}{m} \sum_{i=1}^m P_i} \quad (4)$$

where m and n are number of peaks and trough respectively, P_i is the amplitude of the i th peak and T_j is the amplitude value of the j th trough of the of last two lines. The obtained contrast values are tabulated in Table.I. From this table it is seen that OSEM helps increase the contrast of the reconstructed images by suppressing noise. Since upsampling by USL and URL method can introduce noise, we studied the spectra of a noisy ROI in these images. The 41×41 ROI and the obtained amplitude spectra (with dc suppression) are shown in Fig.9. The URL introduces less noise than USL as evident from the circularly symmetric pattern of the former spectra

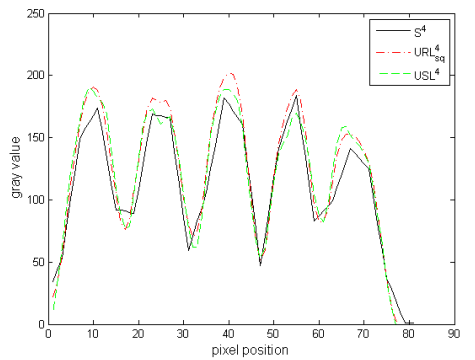
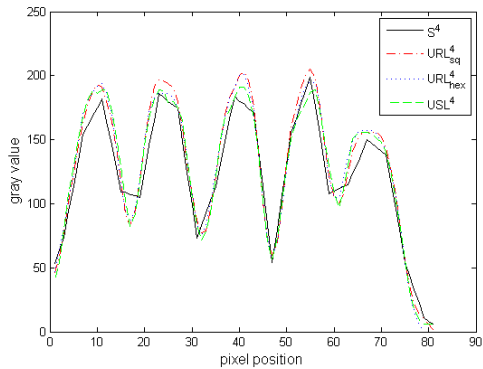
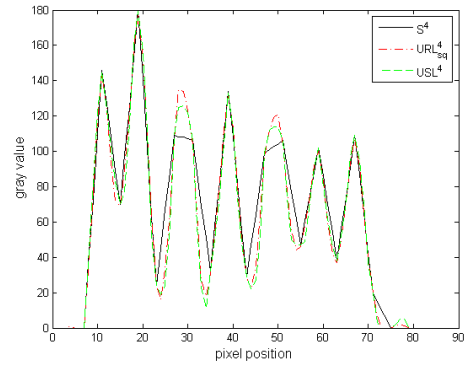
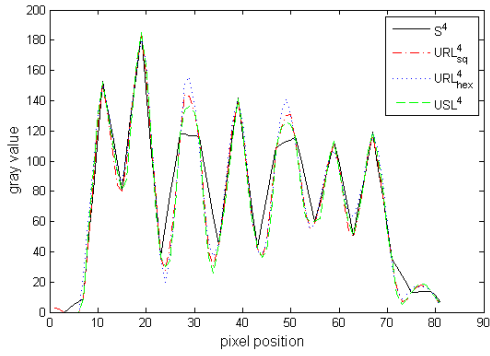
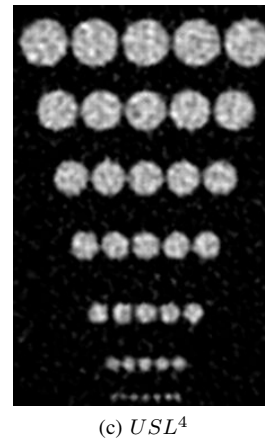
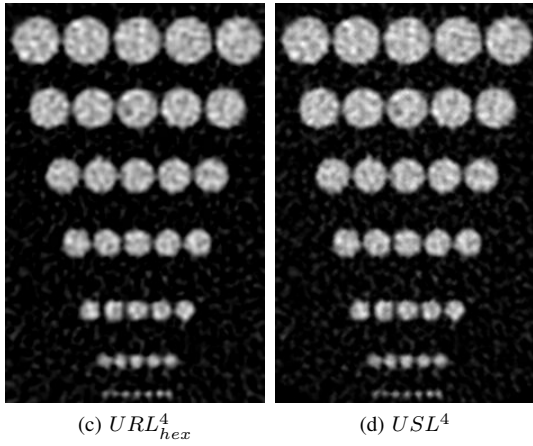
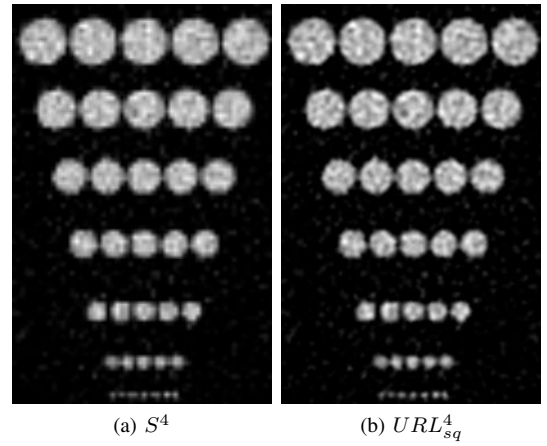
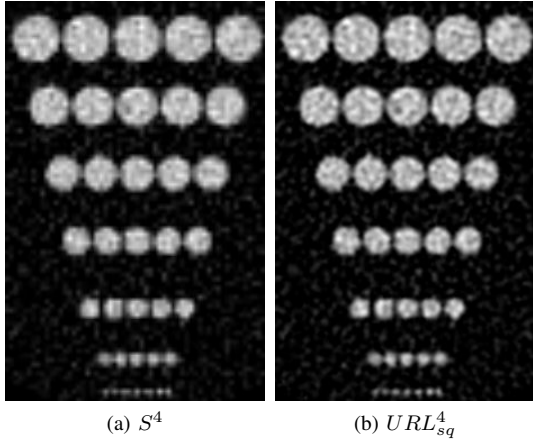


Fig. 7: FBP- based upsampled ($k=4$) results ((a) through (d)) and line profiles of the last two rows for Dots.

Fig. 8: OSEM- based upsampled ($k=4$) results ((a) through (c)), and line profiles of the last two rows for Dots

compared to the wider bandwidth of the spectra in the case of USL. Prominent distortion in line profile for penultimate row of dots also suggests that noise content in USL more than URL. In our experiment we also investigated upsampling by a factor of six. This was to study the relative degradation in quality of the results produced by the different upsampling methods. The results are shown only for the last two lines of dots shown in Fig. 10. From these results it can be seen that both URL and USL are capable of preserving the definition of the circular structures for $k = 6$ compared to S. The results are smoother than direct upsampled result, but are of similar quality with similar distortions in the shapes. However, it should be noted that this similar quality has been obtained in URL with only two images as opposed to six images for USL. From analysis of line profile and contrast ratio, we can conclude that URL generates comparable quality image as USL at lower computational cost.

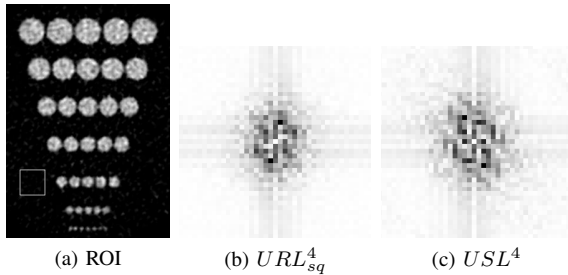


Fig. 9: A noisy ROI of Dots phantom and its noise spectra

V. DISCUSSION AND CONCLUSION

In this paper, we have proposed a new method for generating up-sampled tomographic images which uses samples from two rotated lattices. The results of the proposed method were compared against ISR-2 algorithm [5] and direct up-sampling. Results show that the our scheme produces an image of better quality when compared with direct up-sampling method as well as of comparable quality to the image obtained with ISR-2 algorithm.

Theoretically, for generating k times upsampled image k^2 shifted images are needed. To decrease the computational cost Chang [5] proposed two new algorithm ISR-1 and ISR-2 which require $2k - 1$ and k images respectively without affecting the quality of up-sampled images. Our proposed method offers further reduction as only two images are needed for any up-sampling ($k=2,3,4,\dots$) factor. This amounts to considerable savings in computational cost and storage space.

The main objective of generating upsampled images by combination of low resolution images is to improve the quality and suppress imaging artifacts. Our results (images, spectra and energy distribution plots) demonstrated that URL is able to suppress imaging far more effectively than USL. Part of the reason for this could be the sample distribution that underlies USL (periodic) versus URL (quasi-periodic). This needs further investigation from a sampling theory perspective and to determine the optimal rotation and the best interpolation

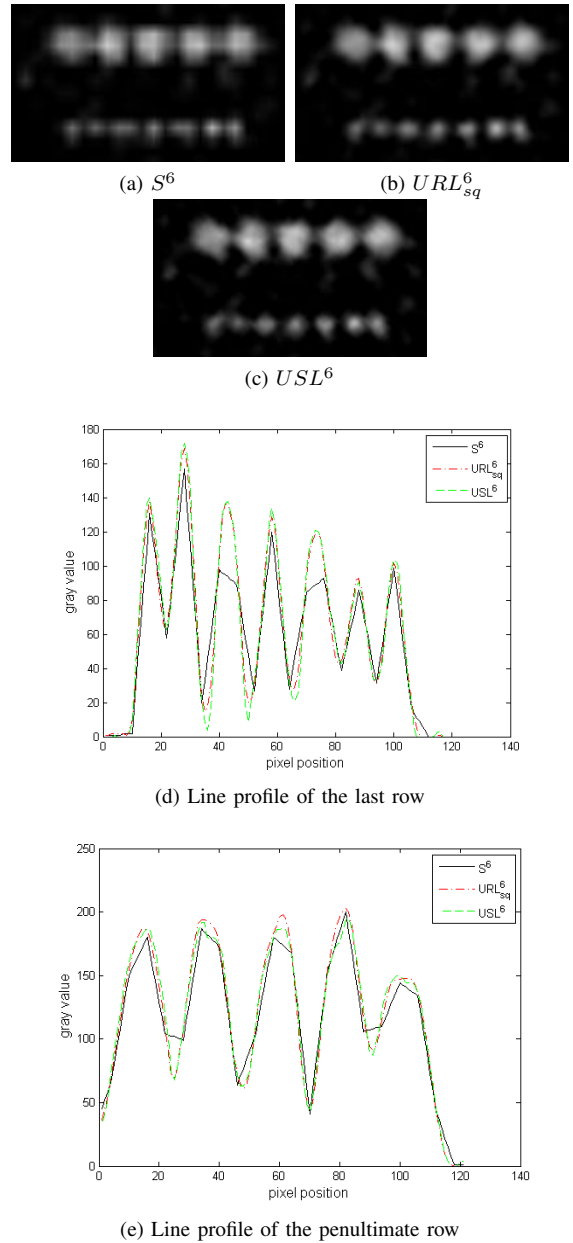


Fig. 10: OSEM-based upsampled ($k=6$) results for Dots displaying last two rows of dots and the corresponding line profiles

kernel to further improve the URL based synthetic zooming scheme.

REFERENCES

- [1] H.Behrmard, "Reconstruction of 2-D signals from union of shifted lattices", *Proc. ICASSP*, vol. 4, 2005, pp 197-200.
- [2] S.H.Izen, D.P.Rohler and K.L.A. Sastry, "Exploiting symmetry in fan beam CT: Overcoming third generation undersampling" *SIAM J. Appl Math*, vol.65, 2005, pp 1027-1052.
- [3] J.Kennedy, O.Israel, A.Frenkel, R.Bar-Shalom, and H.Azhari, "Super-resolution in PET imaging" *IEEE Trans Medical Imaging* vol. 25, 2006, pp 137-147.
- [4] G.Chang, T.Pan, J.Clark, Jr, OR Mawlawi, "Comparison between two super-resolution implementations in PET imaging", *Med. Phys* vol. 36, 2009, pp 1370-1383.

- [5] G.Chang, T.Pan, J.Clark, Jr, OR Mawlawi, "Optimization of super-resolution processing using incomplete image sets in PET imaging" , *Med. Phys* vol. 35, 2008, pp 5748-5757.
- [6] A.Yabushita,K.Ogawa. "Image reconstruction with hexagonal grid" , *Nuclear science symposium*, vol. 3, 2002, pp 1500-1503.
- [7] M.Knaup, S.Steckmann, O.Bockenbach, M. Kachelrie ,"CT image reconstruction using hexagonal grid", *Nuclear science symposium*, Vol 4, 2007, pp 3074-3076.
- [8] N.B. Nill and B.H. Bouzas, "Objective Image Quality Measure Derived from Digital Image Power Spectra", *Optical Engineering*, vol.31, pp.813-825, April 1992.
- [9] Jiri Jan , "Medical image processing, reconstruction, and restoration: concepts and methods", CRC Press, 1006.
- [10] A. C. Kak and Malcolm Slaney, *Principles of Computerized Tomographic Imaging*, IEEE Press, 1988.
- [11] P.Vandewalle, K.Krichane, P.Zbinden, Super resolution toolbox (<http://lcavwww.epfl.ch/software>)
- [12] J.A.Fessler, image reconstruction toolbox (<http://www.eecs.umich.edu/fessler/code>)